

# Rapid Kimberlite Ascent and the Significance of Ar-Ar Ages in Xenolith Phlogopites

S. P. Kelley\* and J.-A. Wartho

Kimberlite eruptions bring exotic rock fragments and minerals, including diamonds, from deep within the mantle up to the surface. Such fragments are rapidly absorbed into the kimberlite magma so their appearance at the surface implies rapid transport from depth. High spatial resolution Ar-Ar age data on phlogopite grains in xenoliths from Malaita in the Solomon Islands, southwest Pacific, and Elovoy Island in the Kola Peninsula, Russia, indicate transport times of hours to days depending upon the magma temperature. In addition, the data show that the phlogopite grains preserve Ar-Ar ages recorded at high temperature in the mantle, 700°C above the conventional closure temperature.

Kimberlites and related types of eruption are composed of a mélange of magma and rock fragments (xenoliths), broken and mixed by turbulent magmatic emplacement. The xenoliths interact with the magma, but many survive intact, thus providing clues of their original lower crustal or mantle chemistry and mineralogy. Foremost among the questions posed by these intrusions is how they bring the xenoliths (and diamonds) to the surface sufficiently quickly to prevent complete absorption. The distances traveled by the deepest xenoliths are inferred to be up to 400 km (1), although recently xenoliths from an alnöite (a kimberlite relative) on Malaita have indicated derivation from 400 to 670 km depth (2). Recent studies of garnet dissolution in kimberlitic magmas have indicated times of only a few hours for transport from the mantle to the surface (3). Argon diffusion in phlogopite mica, the most common potassic mineral in kimberlite systems, provides an alternative approach to constraining travel times.

Because phlogopite generally retains Ar only below 480°C, K-Ar and Ar-Ar bulk mineral dating has been applied to small phlogopite grains in order to measure eruption ages. The ages yielded by large phlogopites from xenoliths are, however, commonly older than the eruption, a phenomenon that has been interpreted as the incorporation of excess radiogenic Ar from a deep fluid source (4–6). In contrast, Pearson *et al.* (7) speculated that phlogopites in xenoliths from the Udachnaya kimberlite retained ages of metasomatism in the Siberian lithospheric mantle. This latter interpretation requires the quantitative retention of radiogenic Ar in the upper mantle, 700°C above the conventional closure temperature, and that the ubiquitous Ar loss profiles at the grain margins

reflect outgassing after incorporation in the kimberlitic magma.

Testing the quantitative retention of radiogenic Ar in phlogopites is dependent upon obtaining samples with good isotopic age constraints. We have overcome this problem by analyzing xenoliths formed during well-characterized magmatic or metasomatic events on Elovoy Island in the Kola Peninsula, Russia, and on Malaita in the Solomon Islands. The Elovoy xenolith was derived from parts of the lower crust formed at 2000 to 2500 million years ago (Ma), during ancient plume events (8). The Malaita xenolith was brought to the surface in an alnöite eruption similar to the one which recently yielded ultradeep xenoliths (2). The age of the lithospheric mantle from which the sample was derived is constrained because it formed during the Ontong-Java plume event at 121 Ma, based on Ar-Ar dating of the flood basalts (9). The two samples thus represent extremes, one derived from ancient lower continental crust and one from younger oceanic lithosphere.

The samples were analyzed using the ultraviolet (UV) laser technique for Ar-Ar dating (10) to achieve high spatial resolution. Narrow trenches were ablated parallel to phlogopite grain margins at a spatial resolution of 10 to 15  $\mu\text{m}$ , and core ages were analyzed using square raster pits (Fig. 1A) (10). The results (5) from both phlogopite samples (Fig. 1, B and C) showed the old cores and young margin pattern seen elsewhere (6). The cores of phlogopites from Malaita (Fig. 1B) and Elovoy Island (Fig. 1C) yielded ages corresponding to the magmatic/metamorphic events dated using other radiogenic isotopes. Moreover, in common with other xenolith phlogopites, they exhibited Ar diffusive loss profiles of similar lengths (200 to 300  $\mu\text{m}$ ) with ages decreasing to the known eruption age at the grain margin (Fig. 1, B and C). This is a characteristic of partially reset ages (11) rather than gain of excess Ar (12). In both cases, the geological history of the xenolith

source rocks is relatively simple (8, 9) and the correspondence of phlogopite core ages with the ages for other known events is not coincidental, considering the difference in the locality and age of the samples. The implication of this result is that Ar loss at the phlogopite grain margins records not a late-stage phenomenon but the integrated time and temperature history of the xenolith transport from depth to the surface.

Using experimentally determined diffusion rates for Ar in phlogopite (13), we can calculate transport times, given estimates of the magma temperatures (Fig. 2). Although the actual magma temperatures are difficult to estimate, the majority of Malaita xenoliths were formed at 1200° to 1300°C (14). However, in the Malaita alnöite, the magma temperatures were considerably lower, as indicated by later crystallized clinopyroxenes (15), perhaps as low as 1000°C. Assuming temperatures in the range of 1200° to 1000°C, the Malaita sample indicates transport times of 13 hours to 11.6 days, and the Elovoy Island sample indicates 8 hours to 289.4 days. These estimates are in line with garnet dissolution experiments, which indicate transport times of less than 1 hour at 1200°C and 1 to 10 hours at 1000°C (3), because Ar loss would continue to lower temperatures and would be expected to indicate longer times. Note that the estimates from garnet dissolution and Ar loss approach each other at higher temperatures, which are expected to dominate the processes given the Arrhenius relationship in both cases (Fig. 2). The phlogopite mica data indicate transport rates of 0.1 to 4  $\text{ms}^{-1}$ , with the slower rates indicated for the Elovoy lamprophyric intrusion. Kimberlites that preserve diamonds may fall toward the higher end of this range.

The other aspect of these results is that phlogopites retained Ar while remaining many hundreds of degrees above their closure temperatures of 400° to 480°C (13, 16) for extended periods of time. We have considered two possible causes for the retention of radiogenic Ar at such high temperatures: anomalously high Ar closure temperatures in the phlogopites or lack of Ar transfer to other phases along the grain boundary network. Experimental data (17) suggest that phlogopites do have variable closure temperatures but only over a few tens of degrees, which is insufficient to explain the preservation of old ages in the mantle. On the other hand, the relatively high solubility of Ar in tri-octahedral micas (biotite and phlogopite) (18) is well documented (19, 20). Thus, Ar will partition into phlogopite in preference to other more tightly packed mineral lattices such as olivine, garnet, or clinopyroxene. Another crucial piece of evidence comes from a study of excess Ar in dry granulites (19), which showed that in K-feldspar-bearing granulites containing small amounts of biotite, excess Ar in biotite was correlated with the K-feldspar

Department of Earth Sciences, Open University, Walton Hall, Milton Keynes, MK7 6AA, UK.

\*To whom correspondence should be addressed. E-mail: s.p.kelley@open.ac.uk

## REPORTS

content of the rock. Thus, above the closure temperatures of biotite and K-feldspar, the radiogenic Ar preferentially partitioned into

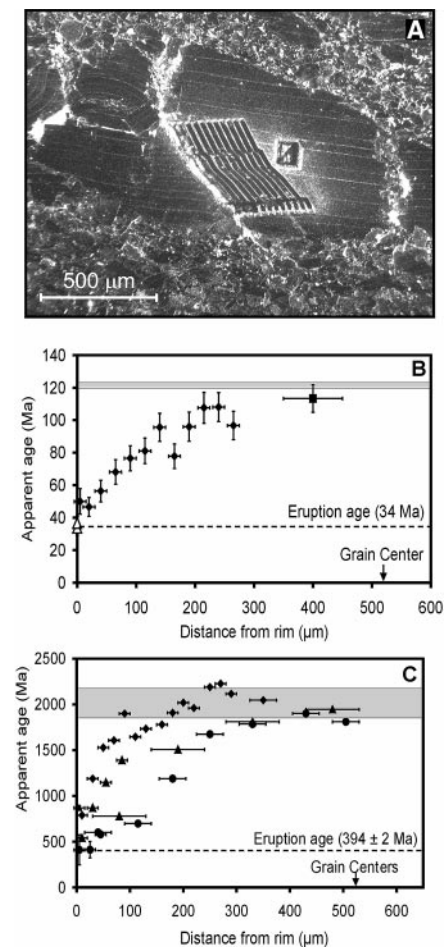


**Fig. 1.** (A) Photomicrograph of UV laser rim-core traverses and square pits in a phlogopite grain from glimmerite sample PHN 4062 from Malaita, Solomon Islands. (B) Plot of apparent Ar-Ar age versus distance for the phlogopite grain shown in Fig. 1A, using UV laser traverse (solid diamonds), 100  $\mu\text{m}^2$  laser pits in core (solid square) and analyses of fine-grained phlogopite matrix (open triangles). The ages at the grain edges are the same as the eruption age of the 34 Ma alnöites, which intrude lavas of the Ontong-Java Plateau (27). Ar-Ar dating of lavas shows that the Ontong-Java Large Igneous Province (LIP) was erupted at  $121.3 \pm 0.9$ ,  $92.0 \pm 1.6$ ,  $\sim 60$ , and  $\sim 34$  Ma (9), though lavas on Malaita have only yielded ages of 121 Ma (28). The grain core age of  $113.3 \pm 8.5$  Ma thus falls within errors of the formation age of the Ontong-Java Plateau at 121 Ma (gray box). (C) Plot of apparent Ar-Ar age versus distance for three grains, using UV laser traverses (solid diamonds, triangles, and circles), of phlogopite sample N-436-11 from a lamprophyre diatreme on Elovoy Island, Kola Peninsula, Russia. The phlogopite grain edge ages correspond with the eruption age of  $394.0 \pm 2.0$  Ma (29). The phlogopites were derived from entrained lower crustal xenoliths from an ancient Palaeoproterozoic LIP formed around 2.4 to 2.5 Ga that underwent K-rich metasomatism associated with a later plume event around 1.7 to 2.2 Ga (gray box) (8).

biotite. By analogy, if one mineral in a rock contains nearly all of the K and also has the highest partition coefficient for Ar, then that mineral will effectively become a closed system.

Stable isotope studies of fluid migration in dry systems, such as high-pressure rocks, indicate that the individual grains do not represent closed systems, because exchange into and transport along the grain boundary network occurs over distances of a few centimeters (21). We can test the extent to which this may be true for the phlogopite ages by estimating a partition coefficient for Ar in this system. A recent pilot study exploring the solubility of Ar in phlogopite yielded values of  $\sim 0.18$  ppm/kPa (22). The grain boundary spaces into which Ar would partition are probably a few nanometers wide (23) and often contain melts, representing around  $2 \times 10^{-6}\%$  of the rock volume (23). The best estimate of Ar solubility in the melt, based on studies at lower pressures, is 2 to 10 ppm/kPa (22, 24). Given these parameters, 0.2 to 1% of the radiogenic Ar would partition into the grain boundary network at equilibrium, and the Ar-Ar phlogopite core ages would approach the age of the most recent fluid or magma flow event in the mantle or lower crust. A further consequence of closed system behavior rather than isotopic closure by cooling is that the individual laser pit ages reflect dynamic equilibrium, and thus areas of higher defect density in the phlogopites may have slightly higher apparent ages, causing the age core variations seen in Fig. 1, B and C.

The wider implication of the retention of Ar in mantle phlogopites over geologically extended periods is that Ar and possibly other noble gases may be stored predominantly in mineral lattices and not in grain boundary networks. Furthermore, other radiogenic noble gases may be immobile in the lithospheric mantle, and

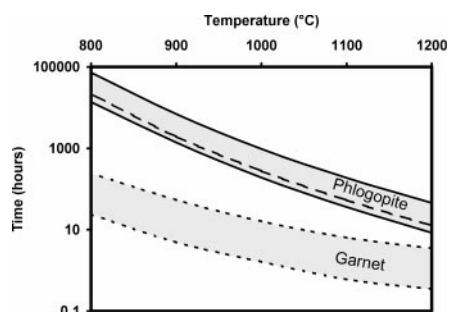


**Fig. 2.** Graph showing travel times for rapid eruptions for a range of assumed magma temperatures. The dashed bordered gray zone refers to the range for garnet dissolution in a Slave Province kimberlite, Canada (3). The dashed line refers to calculations based upon Ar diffusion in phlogopite from an alnöite on Malaita, Solomon Islands. The solid bordered gray zone refers to calculations based on Ar diffusion in phlogopites from Elovoy Island, Kola Peninsula, Russia. Note that the two sets of estimates approach one another to within an order of magnitude at 1200°C.

radiogenic  $^{40}\text{Ar}$ ,  $^4\text{He}$ , and fissionogenic Xe isotopes will correlate with local K, Th, and U abundances. Long residence in closed systems with variable amounts of other incompatible elements may also explain why the heavy noble gas isotope ratios measured in depleted mantle xenoliths can reflect a reservoir similar to that of midocean ridge basalts (25), whereas others reflect a more enriched source (26). Although atmospheric contamination is often evoked as an explanation of such variations, the short eruption time scale indicated by Ar loss profiles constrains the extent of exchange, and the lack of any significant atmospheric  $^{36}\text{Ar}$  influx into the phlogopites during eruption argues against atmospheric contamination. Low Ar isotope ratios measured in subcontinental xenoliths (25) may thus reflect isotope ratio variations within the lithospheric mantle.

### References and Notes

- S. E. Haggerty and V. Sautter, *Science* **248**, 993 (1990); V. Sautter, S. E. Haggerty, S. Field, *Science* **252**, 827 (1991).
- K. D. Collerson, S. Hapugoda, B. S. Kamber, Q. Williams, *Science* **288**, 1215 (2000).
- D. Canil and Y. Fedortchouk, *Earth Planet. Sci. Lett.* **167**, 227 (1999).
- J. F. Lovering and J. R. Richards, *J. Geophys. Res.* **69**, 4895 (1964).
- Web tables of Ar-Ar data are available at [www.sciencemag.org/feature/data/1051550.shl](http://www.sciencemag.org/feature/data/1051550.shl)
- D. Phillips, T. C. Onstott, J. W. Harris, *Nature* **340**, 460 (1989); D. Phillips, *Chem. Geol. Isotope Geosci. Sect.* **87**, 71 (1991).
- D. G. Pearson, S. P. Kelley, N. P. Pokhilenko, F. R. Boyd, *Russ. J. Geol. Geophys.* **38**, 106 (1997).
- P. D. Kempton et al., *J. Petrol.*, in press.
- M. L. G. Tejada, J. J. Mahoney, R. A. Duncan, M. P. Hawkins, *J. Petrol.* **37**, 361 (1996); A. B. Birkhold, C. R. Neal, J. J. Mahoney, R. A. Duncan, *Eos (Fall Suppl.)* **80**, F1103 (1999).
- S. P. Kelley, N. O. Arnaud, S. P. Turner, *Geochim. Cosmochim. Acta* **58**, 3519 (1994).
- S. P. Kelley and G. Turner, *Earth Planet. Sci. Lett.* **107**, 634 (1991).
- C. S. Pickles, S. P. Kelley, S. M. Reddy, J. Wheeler, *Geochim. Cosmochim. Acta* **61**, 3809 (1997).
- B. J. Giletti, in *Geochemical Transport and Kinetics*, Carnegie Institution Publication 634, A. W. Hofmann, B. J. Giletti, H. S. Yoder, R. A. Yund, Eds. (Carnegie Institution, Washington, DC, 1974), pp. 107-115.
- P. H. Nixon and F. R. Boyd, in *The Mantle Sample: Inclusions in Kimberlites and Other Volcanic Rocks*, Proceedings of the 2nd Kimberlite Conference, Santa Fe, NM, 3 to 7 October 1977, N. M. Boyd and H. O. A. Meyer, Eds. (American Geophysical Union, Washington, DC, 1979), pp. 400-423; C. R. Neal and P. H. Nixon, *Trans. Geol. Soc. S. Afr.* **88**, 347 (1985).
- P. H. Nixon, R. H. Mitchell, N. W. Rogers, *Mineral. Mag.* **43**, 587 (1980).
- M. H. Dodson, *Contrib. Mineral. Petrol.* **40**, 259 (1973).
- M. Grove and T. M. Harrison, *Am. Mineral.* **81**, 940 (1996).
- P. S. Dahl, *Contrib. Mineral. Petrol.* **123**, 22 (1996).
- K. A. Foland, *Geochim. Cosmochim. Acta* **43**, 793 (1979).
- J. C. Roddick, R. A. Cliff, D. S. Rex, *Earth Planet. Sci. Lett.* **48**, 185 (1980).
- S. Nadeau, P. Philippot, F. Pineau, *Earth Planet. Sci. Lett.* **114**, 431 (1993); D. Rumble and T. Yui, *Geochim. Cosmochim. Acta* **62**, 3307 (1998).
- K. Roselieb, J.-A. Wartho, H. Büttner, A. Jambon, S. Kelley, 10th European Union of Geosciences Meeting, 28 March to 1 April 1999, Strasbourg, France (*Terra Abstr.* **4**, Cambridge Publications, Cambridge, 1999), p. 368.

23. M. R. Drury and J. D. F. Fitz Gerald, *Geophys. Res. Lett.* **23**, 701 (1996); R. Wirth, *Contrib. Mineral. Petrol.* **124**, 44 (1996).
24. M. R. Carroll, D. S. Draper, R. A. Brooker, S. Kelley, in *Noble Gas Geochemistry and Cosmochemistry*, J. Matsuda, Ed. (Terra Scientific, Tokyo, 1994), pp. 325–341.
25. T. Matsumoto, M. Honda, I. McDougall, S. Y. O'Reilly, *Geochim. Cosmochim. Acta* **62**, 2521 (1998).
26. T. J. Dunai and H. Baur, *Geochim. Cosmochim. Acta* **59**, 2767 (1995).
27. G. L. Davies, *Carnegie Inst. Wash. Yearb.* **76**, 631 (1977).
28. C. R. Neal et al., in *Large Igneous Provinces: Continental, Oceanic, and Planetary Flood Volcanism* (*Geophys. Monogr.* **100**, American Geophysical Union, Washington, DC, 1997), pp. 183–216.
29. A. D. Beard et al., *Lithos* **39**, 93 (1996).
30. We thank G. Pearson (Durham University, UK) for kindly providing the samples from Malaita and H. Downes (Birkbeck College, University of London) and P. Kempton (UK National Environment Research Council Isotope Unit) for providing the sample from Elovoy Island. S.P.K. and J.-A.W. greatly appreciate a grant from the Leverhulme Trust that allowed this work to be undertaken.

21 April 2000; accepted 12 June 2000

# A Potent Greenhouse Gas Identified in the Atmosphere: SF<sub>5</sub>CF<sub>3</sub>

W. T. Sturges,<sup>1</sup> T. J. Wallington,<sup>2</sup> M. D. Hurley,<sup>2</sup> K. P. Shine,<sup>3</sup> K. Sihra,<sup>3</sup> A. Engel,<sup>4</sup> D. E. Oram,<sup>1</sup> S. A. Penkett,<sup>1</sup> R. Mulvaney,<sup>5</sup> C. A. M. Brenninkmeijer<sup>6</sup>

We detected a compound previously unreported in the atmosphere, trifluoromethyl sulfur pentafluoride (SF<sub>5</sub>CF<sub>3</sub>). Measurements of its infrared absorption cross section show SF<sub>5</sub>CF<sub>3</sub> to have a radiative forcing of 0.57 watt per square meter per parts per billion. This is the largest radiative forcing, on a per molecule basis, of any gas found in the atmosphere to date. Antarctic firn measurements show it to have grown from near zero in the late 1960s to about 0.12 part per trillion in 1999. It is presently growing by about 0.008 part per trillion per year, or 6% per year. Stratospheric profiles of SF<sub>5</sub>CF<sub>3</sub> suggest that it is long-lived in the atmosphere (on the order of 1000 years).

The Kyoto Protocol highlighted the need to assess a broad range of greenhouse gases for their contribution to radiative forcing. Whereas most attention has been placed on the major greenhouse gases (CO<sub>2</sub>, CH<sub>4</sub>, and N<sub>2</sub>O), it is clear that some gases that are present at much lower concentrations can contribute to global warming because of their exceptionally large infrared (IR) absorption. A notable example is SF<sub>6</sub>, which is closely chemically related to the "new" molecule SF<sub>5</sub>CF<sub>3</sub>. SF<sub>6</sub> is of almost exclusively anthropogenic origin, currently present in the atmosphere at only ~4 parts per trillion (ppt), but with a global warming potential (GWP) of 22,200 relative to CO<sub>2</sub> over a 100-year time horizon (1). SF<sub>6</sub> is one of the greenhouse gases that the Kyoto Protocol seeks to control.

We first noted SF<sub>5</sub>CF<sub>3</sub> as an unidentified chromatographic peak that eluted shortly after SF<sub>6</sub> in gas chromatography–mass spectrometry (GC-MS) analysis of stratospheric air samples. The identity of the peak was determined by the presence of ions with masses of 68.995 (CF<sub>3</sub><sup>+</sup>), 88.967 (SF<sub>3</sub><sup>+</sup>), and

126.964 (SF<sub>5</sub>CF<sub>3</sub><sup>+</sup>) in their correct relative abundances, and the identity was then confirmed by an exact GC retention time match with a sample of pure compound (from Flura Corporation, Newport, Tennessee) diluted in nitrogen. The mass spectrum (comprising almost exclusively the three above-mentioned ions) was obtained from the pure compound because no library spectrum could be found.

Air samples were analyzed with the GC-MS system operated in single-ion mode (a mass of 88.967 was used to monitor SF<sub>5</sub>CF<sub>3</sub>), giving a detection limit of ~1 part per 10<sup>15</sup> for 800-ml air volumes (2, 3). SF<sub>6</sub> concentrations were referenced to a calibrated ambient air standard (Colorado Mountains, 1994; SF<sub>6</sub> = 3.39 ppt) (4). SF<sub>5</sub>CF<sub>3</sub> was calibrated by two separate methods (5), giving a mean concentration in the same air standard of 0.094 ± 0.020 ppt.

Samples of air were pumped out of deep consolidated snow (firn) at Dome Concordia in eastern Antarctica (75°S, 123°E; 3233 m above sea level) in January 1999 (6) at various depths from the surface to pore close-off at ~100 m. Mean equilibration times between changing surface concentrations and air at depth in the firn can be on the order of years or even decades, depending on the diffusivity of the particular gas and its concentration gradient. This was calculated with the aid of a diffusive transport model constrained by measured profiles of gases with well-known atmospheric trends (e.g., CO<sub>2</sub>) (7).

Profiles of SF<sub>5</sub>CF<sub>3</sub> and SF<sub>6</sub> with depth in

the firn are shown in Fig. 1. They are remarkably similar in form, leading to the suspicion that their growth rates are closely related. Published measurements and emission estimates for SF<sub>6</sub> were combined (8) to give the global SF<sub>6</sub> trend shown in the inset of Fig. 1. Modeling this trend gave an excellent match to the observed SF<sub>6</sub> concentrations in the firn, except for a possible slight overestimate from extrapolating the trend from 1997 to 1999. A hypothetical trend for SF<sub>5</sub>CF<sub>3</sub> was then constructed with the SF<sub>6</sub> trend scaled to the mean relative concentration of SF<sub>5</sub>CF<sub>3</sub> to SF<sub>6</sub> in surface air at Dome Concordia (0.122 to 4.00 ppt) (Fig. 1). This trend was modeled with a diffusion coefficient for SF<sub>5</sub>CF<sub>3</sub> in air estimated from molecular volume calculations (9). The resulting fit to the observed SF<sub>5</sub>CF<sub>3</sub> profile is very good (Fig. 1), with most measurements falling within an envelope of concentrations 10% above and below the mean. We therefore think that this time trend for SF<sub>5</sub>CF<sub>3</sub> is a good representation of its actual atmospheric growth and suggests that emissions began in the late 1950s.

Air was also collected from the stratosphere by using a balloon-borne liquid neon-based cryogenic sampler (10). Vertical profiles of SF<sub>5</sub>CF<sub>3</sub> are shown in Fig. 2 for both mid-latitude and Arctic vortex flights, launched from Aire sur l'Adour, France (44°N), and Kiruna, Sweden (68°N), respectively. At both latitudes, the concentrations declined monotonically with altitude. Measurements of SF<sub>6</sub> were used to determine the mean age of air (11) for each sample. The mean ages at maximum altitude were 4 and 7 years for the mid-latitude and Arctic vortex flights, respectively. The greater decline in SF<sub>5</sub>CF<sub>3</sub> with altitude observed for the high-latitude flight can be explained by subsidence of older air in the polar vortex. The SF<sub>5</sub>CF<sub>3</sub> concentrations expected on the basis of the mean age of air and the atmospheric trend of SF<sub>5</sub>CF<sub>3</sub> (from Fig. 1) are shown as thick lines in Fig. 2. Agreement between the predicted and measured SF<sub>5</sub>CF<sub>3</sub> is very good within the errors of the measurements, at least at lower altitudes. We therefore expect the upper limit of the lifetime of SF<sub>5</sub>CF<sub>3</sub> to approach that of SF<sub>6</sub> [3200 years (12)]. By analogy with SF<sub>6</sub>, we do not expect any substantial sinks of SF<sub>5</sub>CF<sub>3</sub> in the troposphere nor do we expect uptake by soils, plants, or the ocean (12).

Toward the top of the stratospheric profiles (Fig. 2), there is evidence of a possible divergence toward observed SF<sub>5</sub>CF<sub>3</sub> concentrations

<sup>1</sup>School of Environmental Sciences, University of East Anglia, Norwich NR4 7TJ, UK. <sup>2</sup>Ford Motor Company, Mail Drop SRL-3083, Dearborn, MI 48121-2053, USA. <sup>3</sup>Department of Meteorology, University of Reading, Reading RG6 6BB, UK. <sup>4</sup>Institute for Meteorology and Geophysics, Johann Wolfgang Goethe University of Frankfurt, D-60325 Frankfurt, Germany. <sup>5</sup>British Antarctic Survey, Natural Environment Research Council, Cambridge CB3 0ET, UK. <sup>6</sup>Atmospheric Chemistry Division, Max Planck Institute for Chemistry, D-55060 Mainz, Germany.